

## Modeling of Monthly Meteorological Time Series

Azumah Karim<sup>1</sup>, Ananda Omotukoh Kube<sup>2</sup> and Bashiru Imoro Ibn Saeed<sup>3</sup>

### Abstract

The average monthly temperature and rainfall time series recorded between January, 1991 to December, 2016 in five selected African countries climatic zones (Ghana, Kenya, Namibia, Egypt and Cameroon) from West Africa, East Africa, Southern Africa, Northern and the Central Africa respectively, obtained from the World Bank Group Climate Change Knowledge Portal, were modeled and fitted. In this study, we used the Fourier function with seasonal autoregressive integrated moving average, seasonal autoregressive integrated moving average process, and natural cubic splines to capture the dynamics of the time series data. The Fourier function with seasonal autoregressive integrated moving average; FARIMA approach produce the best fitting models for average monthly temperature and averagely monthly rainfall for selected study countries in Africa.

**Keywords:** Fourier Function; Time Series; Regression; Splines

---

<sup>1</sup> Pan African University, Institute for Basic Sciences, Technology and Innovation, Kenya.

<sup>2</sup> Kenyatta University, Kenya.

<sup>3</sup> Kumasi Technical University, Ghana.

## 1 Introduction

The modeling of the forthcoming progressions of meteorological measures using past time series data is fundamental for environmental sciences, agricultural and agribusinesses or other natural sciences as well as climate modeling, [1, 2]. These models are used to analyze components in trends, seasonally and cyclical in particular times, used in simulating future forecasts of climate and inputs to crop production models. Accordingly [3], adopted time series modeling in investigating the relationship between economic growth and environmental quality. Also [4, 5] employed similar time series approaches to study on the amount of rainfall from historical rainfall data to investigate potential changes in rainfall volumes between 1981 - 2010. Over the period in particular the used of seasonal autoregressive integrated moving average has gained grounds as the appropriate method for modeling environmental time series factors. The Intergovernmental Panel on Climate Changes (IPCC) fourth and fifth assessment reports, indicated that Global climate has seen an extreme change during the last century and its expected to continue on this observed pattern for the future. Consequently, affecting global patterns of climate indicators, such as extreme rainfall, precipitation, humidity, and temperature. In crop production models the role of climatic and as well as environmental factors cannot be over emphasized, [6, 7, 8, 9, 10, 11] and as it stated by [1] meteorological time series models should be considered in climatic modeling. An increasing temperature couple with decreasing rainfall volumes are fundamental contributing factors to severe extreme environmental conditions, such as food security, drought, flooding and depletion of fish stocks in the water bodies are partly responsible for global climate change, [12, 13, 14, 15, 16, 17]. Several times series analysis and predictions models relied on past or historical data. Assuming that the past distributions of the data are capable of modeling of the future outcomes. Recently, one of common identifiable time series model is the seasonal autoregressive integrated moving average (SARIMA) modeling. Ensuring that the historical data are adequate in forecasting future development with certainty. A time series is composed of the following components, namely; trend, seasonal, cyclical and the irregular components. The used of these approaches are vast in the literature, [18, 19, 20, 21, 22, 23]. In addition, regression modeling are enormously considered in modeling climate



maxima regime occurring south of latitude  $8^{\circ}30'N$ , with two maximum periods occurring from May to August and from September to October; and (b) the single maximum regime found north of latitude  $8^{\circ}30'N$ , where there is only one rainy season from May to October, followed by a long dry season from November to May. In northern Ghana, the wet season occurs between May and November, when the Inter-Tropical Convergence Zone (ITCZ) is in its northern position and the prevailing wind is southwesterly, and the dry season occurs between December and March, when the "Harmattan" wind blows northeasterly. The south-eastern coastal strip is dry and different from the north and the south. The seasonal rainfall in the region varies considerably on interannual and inter-decadal timescales, due in part to variations in the movements and intensity of the ITCZ, and variations in timing and intensity of the West African monsoon. The most predictable cause of these variations is the El Niño Southern Oscillation (ENSO). El Niño events are associated with drier than average conditions in West Africa. Seasonal variations in temperature in Ghana are greatest in the north, with highest temperatures in the hot, dry season (April, May, and June) at  $27 - 30^{\circ}C$ ; further south, temperatures are lower (June, August, September) at  $22 - 25^{\circ}C$ .

Kenya's climate ranges from tropical (along the coast) to arid (in the mountain regions). Kenya's climate is impacted by the El Niño Southern Oscillation (ENSO), as well as the movement of the Inter-Tropical Convergence Zone (ITCZ). The rainy season in Kenya usually begins in March and decreases in May to June. The second wet season begins around September/October and shows a decreasing trend in December. The windiest time of the year occurs during the southeast monsoon, which extends from May to September. Kenya normally experienced its dry season between June to October. During the dry season daytime temperatures are usually around  $23^{\circ}C$  at higher altitudes, such as the Masai Mara, and  $28^{\circ}C$  at lower altitudes, such as the coastal areas. From June to October, the country experienced its coldest months. Whereas the wet season is from November to May. The wet season daytime temperatures are between  $24^{\circ}C$  and  $27^{\circ}C$  at higher altitudes. At lower altitudes daytime temperatures are more consistent and hover around  $30^{\circ}C$ . A period of unpredictable, short rains between November and December that lasts about a month. A dry spell in the rainy season occurs between January and February with less rainfall. From March to May the country get the most

rain.

Namibia has a sub-tropical climate, desert along the coast and in the south, and arid, but with a rainy season from November to March, in inland north-central areas and in the north-east. The driest region is the coastal area, where the Namib Desert is located, as well as the south, where the Kalahari Desert is found. The latter is slightly rainier and the rainiest area of Namibia is the north-east, where rainfall ranges from 500 to 600 millimeters per year. Winter is dry everywhere, while in non-desert regions (north and east) it rains in summer, from November to March, usually in the form of showers or thunderstorms in the afternoon. The peak of the rainy season is from January to March.

Egypt annual average temperatures increase from about  $20^{\circ}\text{C}$  on the Mediterranean coastline to around  $24^{\circ}\text{C}$  on the Red Sea coastline,  $25^{\circ}\text{C}$  at Cairo, and  $26^{\circ}\text{C}$  further south at Aswan. Typical daytime maximum temperatures in midsummer range from  $30^{\circ}\text{C}$  at Alexandria southward to  $41^{\circ}\text{C}$  at Aswan; while the corresponding north-south range in midwinter daytime maximum temperatures is  $18\text{-}23^{\circ}\text{C}$ . There have been widespread warming trends over Egypt since 1960 with greater warming in summer ( $0.31^{\circ}\text{C}$  per decade) than during winter ( $0.07^{\circ}\text{C}$  per decade); statistical confidence is higher for the summer warming trend. Between 1960 and 2003, there has been an increase in the frequency of warm nights and a decrease in the frequency of cool nights, and a general increase in average summer temperatures. Nighttime temperatures (daily minimum) show a widespread positive shift in the distribution with fewer cool nights and more warm nights. Confidence is high throughout. Rainfall variability within Egypt is almost inconsequential, given that the country receives very little rainfall, as well as the fact that its agriculture is irrigated and not rain-fed. Variability in Nile flows are moderated by the High Aswan Dam. The dam has one years worth of storage capacity, to help in handling periodic droughts, although Egypt remains vulnerable to multiyear droughts

Cameroon has one main rainy season that lasts from May-November when the West African Monsoon brings moist air over the country from the Atlantic Ocean. The peak rainy months correspond with the lowest average temperatures of the year. The Southern Plateaus experience two shorter rainy seasons during May-June and October-November. Cameroons dry season lasts from

December-April and corresponds with the highest average temperatures of the year during the latter part of the season in the months of February-April. The southern part of the country is characterized as humid and equatorial with temperatures ranging from 20-25°C (depending on altitude) and the wettest regions receiving more than 400 mm of rainfall per month. Northern Cameroon (north of 6°) is semi-arid and dry with temperatures ranging from 25-30 °C. This portion of the country receives less than 100 mm of rainfall per month. The meteorological time series variables were obtained from World Bank Climate Change Knowledge Portal (CCKP), an online tool that provides access to comprehensive global and country data information related to climate change and development on monthly average temperature and rainfall of the five selected countries in the African continent for period 1991 to 2016. The open R source is employed in analyzing the data.

Table 1: Descriptive statistics of the monthly average (1991-2016) meteorological time series variables from five African countries

Meteorological Variables	Country	Mean	Min	Max	Stds	Median	Skewness	Kurtosis
Temperature(0 C)	Ghana(GHA)	27.63	24.99	31.08	1.48	27.35	0.41	2.10
	Kenya(KEN)	25.12	22.78	27.75	1.08	25.16	0.04	2.40
	Namibia(NAM)	21.00	13.09	26.86	3.66	22.23	-0.44	1.78
	Egypt(EGY)	23.06	11.85	32.03	6.24	24.20	-0.24	1.57
	Cameroon(CMR)	24.93	22.95	27.96	1.17	24.60	0.61	2.25
Rainfall(MM)	Ghana(GHA)	96.06	0.00	243.27	64.30	107.47	0.02	1.76
	Kenya(KEN)	54.80	1.16	247.08	39.56	43.82	1.46	5.53
	Namibia(NAM)	22.70	0.03	180.70	29.25	7.98	1.71	6.50
	Egypt(EGY)	2.49	0.14	20.20	2.29	1.78	2.75	15.89
	Cameroon(CMR)	131.52	3.52	387.33	90.35	134.32	0.26	2.06

Descriptive statistics of these variables on the various countries are presented on Table 1, it indicates that, the highest mean and median temperature under consideration were recorded in Ghana and the least in Namibia. The temperature variables are characterized by positive and negative skewness and small kurtosis observed in Table 1, an indication of a skewed distributions. However, an entirely separate distribution is observed for rainfall under consideration. With positive skewness and high kurtosis except that of Ghana and Cameroon, indicating a right skewed peaked distributions.

### 3 Methods

A time series signal is normally generated by ordered sequence of values with time, usually a stationary process or a nonstationary process, that is, either a white noise, an autoregressive, a moving average, an ARMA process or a mixed integrated processes. Environmental Time series modeling is aimed at developing a suitable model to describe and explain inherent structure of the series, purposely for prediction, monitoring, and controlling or guiding to facilitate a codified decision making. These models were propagated by [26, 27, 28, 29].

**Definition 3.1. Moving Average processes:** A Moving Average model is that constructed by simple linear combination of lagged elements of purely random process  $\varepsilon_t$  with  $E(\varepsilon_t) = 0$ . A moving average process,  $(X_t)$  of order  $q$  is defined by:

$$X_t = \beta_0\varepsilon_t + \beta_1\varepsilon_{t-1} + \dots + \beta_q\varepsilon_{t-q} = \sum_{i=0}^q \beta_i\varepsilon_{t-i} \quad (1)$$

denoted as  $MA(q)$

**Definition 3.2. Autoregressive Processes:**

Supposed that  $\{\varepsilon_t\}$  is a purely a random process with mean zero and variance  $\sigma_\varepsilon^2$ . Then the process  $\{X_t\}$  is said to be an autoregressive process of order  $p$ , denoted as  $AR(p)$  and defined as:

$$X_t = \alpha_1X_{t-1} + \alpha_2X_{t-2} + \dots + \alpha_pX_{t-p} + \varepsilon_t \quad (2)$$

**Definition 3.3. Autoregressive moving average (ARMA) process:**

The general autoregressive moving average process with  $AR$  order  $p$  and  $MA$  order  $q$  denoted as  $ARMA(p, q)$ , processes can be written as

$$X_t = \alpha_1X_{t-1} + \alpha_2X_{t-2} + \dots + \alpha_pX_{t-p} + \varepsilon_t + \beta_1\varepsilon_{t-1} + \dots + \beta_q\varepsilon_{t-q} \quad (3)$$

Using the backward shift operator  $\beta$ , equ.(3) may be written in the form

$$\phi(\beta)X_t = \theta(\beta)\varepsilon_t \quad (4)$$

where  $\phi(\beta)$ ,  $\theta(\beta)$  are polynomials of order,  $p, q$ , respectively, such that

$$\phi(\beta) = 1 - \alpha_1\beta - \alpha_2\beta^2 - \dots - \alpha_p\beta^p \quad (5)$$

$$\theta(\beta) = 1 + \beta_1\beta + \beta_2\beta^2 + \dots + \beta_q\beta^q \quad (6)$$

Accordingly for an *AR* process, the values  $\{\alpha_i\}$ , which make the process stationary are such that the roots of  $\phi(\beta) = 0$ , lie outside the unit circle, while for an *MA* process, the values of  $\{\beta_i\}$ , which makes the process invertible are such that the roots of  $\theta(\beta) = 0$ , lie outside the unit circle.

**Definition 3.4. Seasonal Integrated Autoregressive moving average (SARIMA) process:**

A stationary time series  $\{X_t\}$  is defined as a seasonal ARIMA as

$$\Phi_P(B^s)\phi(B)\nabla_s^D\nabla^d X_t = \alpha + \Theta_Q(B^s)\theta(B)\varepsilon_t \quad (7)$$

with  $\varepsilon_t$  as Gaussian white-noise process,  $\phi(B)$  and  $\theta(B)$  as the ordinary autoregressive (AR) and moving average (MA) operators of order  $p$  and  $q$  respectively;  $\Phi_P(B^s)$  and  $\Theta_Q(B^s)$  as seasonal autoregressive (AR) and moving average (MA) operators of order  $P$  and  $Q$  respectively, with seasonal period  $s$ .

To define an appropriate model for a particular time series data, it is essential to obtain the sample autocorrelation function (ACF) and sample partial autocorrelation function (PACF) for examination, which mirror how the observations in a time series are correlated. The plot of ACF helps to determine the order of MA process, and the plot of PACF helps to find order AR process.

For SARIMA modeling, the focal point is deciding on an appropriate ideal order; thus, values  $p, q, P, Q, D, d$ . If  $d$  and  $D$  are identified, we can choose the orders  $p, q, P$  and  $Q$  via one of the forecast measure error: the root mean squared error (RMSE), and mean absolute error (MAE).

### 3.1 Model Comparisons/ discrimination

To discriminate among the models, the forecast performance of each of the models will be compared using forecasting accuracies statistical measures. The Mean Absolute Error (MAE), Root Mean Square Error (RMSE) and the Mean Absolute Percentage Error (MASE). Where lower values of the forecasting

accuracies statistical measures imply better forecast of the model. Given that  $e_t$ , the forecast error is defined as  $e_t = X_t - f_t$  and  $f_t$  as the forecast values,  $n$ , the sample size

**Mean Absolute Error (MAE):**

is defined as

$$MAE = \frac{1}{n} \sum_{t=1}^n |e_t| \quad (8)$$

**Root Mean Square Error (RMSE):**

is defined as

$$RMSE = \sqrt{\frac{1}{n} \sum_{t=1}^n e_t^2} \quad (9)$$

**Mean Absolute Scaled Error (MASE):**

the Mean Absolute Scaled Error as

$$MASE = \left( \frac{MAE}{\Delta} \right) \quad (10)$$

where

$$\Delta = \frac{1}{n-1} \sum_{t=2}^n |x_t - x_{t-1}| \quad (11)$$

or

$$\Delta = \frac{1}{n-s} \sum_{t=s+1}^n |x_t - x_{t-s}| \quad (12)$$

The MASE was offered by [30], for relating prediction accuracies. It is independent of the scale of the data, enabling it to be use for comparing forecasts for data sets with different scales. The forecasting methods with the lowest MASE is the preferred one.

Time series models such as the  $AR(p)$ ,  $MA(q)$ ,  $ARMA(p, q)$ ,  $ARIMA(p, d, q)$  as well as the  $SARIMA(p, d, q)(P, D, Q)_s$  sometimes does not tend to give good results for the time series with a longer period for at least two centuries. To remedied this situation, we employed a regression with ARIMA errors, the regression terms are model with the Fourier functions which is adequate for modeling the inherent structure of the time series data, and the correlated errors with the ARIMA models. The adequate number of the sinusoid for the Fourier terms is determined by using periodogram of the data and the orders of models in the  $SARIMA, p, d, q, P, D, Q$  are obtain by studying ACF and

PACF plots of respective time series signals. To be new specific, we study the ensuing model:

$$X_t = \sum_{k=1}^K (m_k \cos 2\pi f_k t + n_k \sin 2\pi f_k t) + \epsilon_t \quad (13)$$

where  $m_k$  and  $n_k$  are the Fourier coefficients,  $f_k$  are the frequencies,  $t$  is time and  $\epsilon_t$  is SARIMA process model as

$$\Phi_P(B^s)\phi(B)\nabla_s^D\nabla^d\epsilon_t = \alpha + \Theta_Q(B^s)\theta(B)z_t \quad (14)$$

where  $z_t$  is white noise. The  $K$  is the number of sinusoidal term,  $s$  is the length of seasonality.

In this paper, the process will be referred as  $FARIMA(K, p, d, q)(P, D, Q)_s$ . Also, in this study we used Natural cubic spline defined as

$$x_i(t) = a_i(t - t_i)^3 + b_i(t - t_i)^2 + c_i(t - t_i) + d_i \quad 1 \leq i \leq m - 1 \quad (15)$$

Using Truncated Power Basis to model the signal as given in equation (15) is

$$X(t) = \sum_{j=0}^3 \beta_j t^j + \sum_{k=1}^K \theta_k (t - \eta_k)_+^3 \quad (16)$$

where  $\eta_k$  is the knots and  $K$  is number of knots of the data-set. In general the truncated power basis of a function with degree  $r$  and  $K$  knots can be written as

$$X(t) = \sum_{j=0}^r \beta_j t^j + \sum_{k=1}^K \theta_k (t - \eta_k)_+^3 \quad (17)$$

and therefore the cubic spline for time series is modeled using the truncated power basis as

$$X(t) = \sum_{j=0}^3 \beta_j t^j + \sum_{k=1}^K \theta_k (t - \eta_k)_+^3 \quad (18)$$

where

$$(t - \eta_k)_+^3 = \begin{cases} (t - \eta_k)_+^3, & \text{if } (t - \eta_k)_+^3 > 0 \\ 0, & \text{if } (t - \eta_k)_+^3 \leq 0 \end{cases} \quad (19)$$

where  $K$  and  $\eta_k$  are the number of knots and knots position of the data-set. The open source R.3.5.2 version will be employed in analyzing the data.

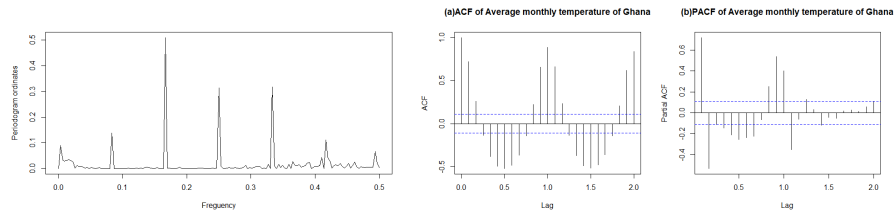
## 4 Results and Discussion

Climatic conditions such as temperature and rainfall data collected in five African sites from different climatic zones are used to build appropriate FARIMA, SARIMA, and NCS models. Quite a lot of authors in the literature have conducted comparable studies in the preceding period, notwithstanding, a majority of the studies primarily deliberated on ARMA, ARIMA or SARIMA models for particular period of time, namely; weekly average, monthly average or yearly average time series. For case in point, [31] modeled Kapsoya historical rainfall data of Uasin Gishu county in Kenya based on  $SARIMA(0, 0, 0)(0, 1, 2)_{[12]}$  ;

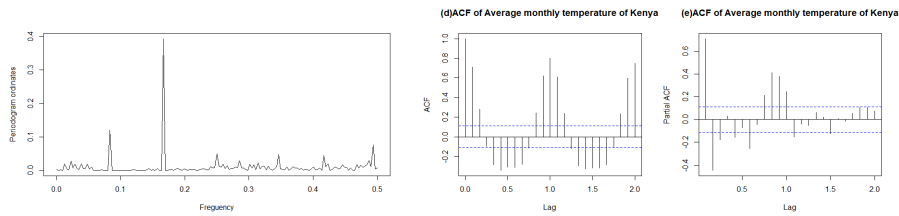
[22] used a first-order differenced  $SARIMA(1, 1, 1)(0, 1, 2)_{[12]}$  a suitable model for predicting rainfall pattern in Embu, County. [25] modeled historical rainfall of Nakuru County and found  $SARIMA(0, 0, 1)(0, 1, 1)_{[12]}$  to be best fitted model. More so, [13] found that, there are significant variations on rainfall and temperature overtime (1986-2015) in Siaya County. Additionally, [18] used the  $SARIMA(0, 0, 0)(2, 1, 0)_{[12]}$  model for forecasting the monthly rainfall of the Ashanti Region of Ghana, while [19] also identified  $SARIMA(0, 0, 0)(1, 1, 1)_{[12]}$  model as an appropriate model for predicting monthly average rainfall figures for the Brong Ahafo Region of Ghana. [12] study revealed that there are fluctuations and an increase in the air temperature for all the twelve months of the study period in Egypt. [32] used SARIMA to model a long term temperature data of Dibrugarh, Assam, for the period of fifty (50) years (1966-2015). Their analysis reveals that the best seasonal models which are satisfactory to describe the data are  $SARIMA(2, 1, 1)(0, 1, 1)_{[12]}$  for monthly maximum and  $SARIMA(2, 1, 1)(0, 1, 1)_{[12]}$  for monthly minimum temperature data respectively.

In this paper, we considered records since January, 1991 to December, 2016 average monthly temperature and rainfall, a total of 312 observation each, to fit the generated statistical models for the average monthly temperature and the rainfall. The plot of the periodograms, and their autocorrelation functions (ACF) and partial autocorrelation functions (PACF), plotted in Figures 2 and 3, were examined to establish the prospective processes of FARIMA and SARIMA models for the monthly average temperature and the rainfall data.

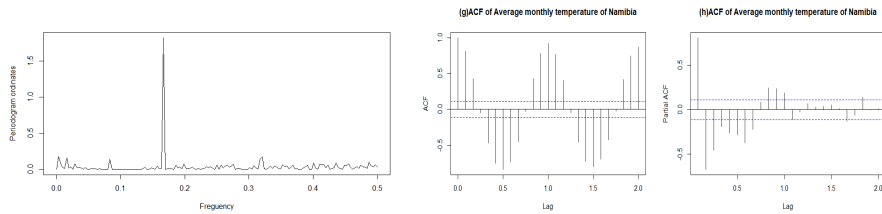
In addition the natural cubic spline was considered for comparative analysis



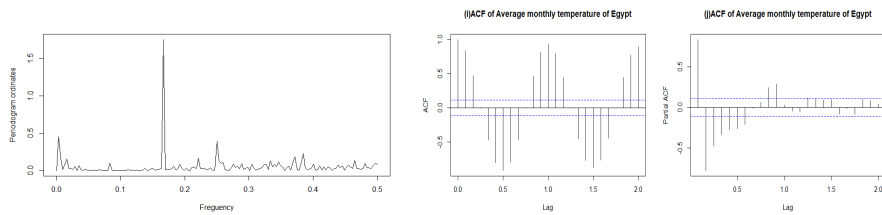
(a) Ghana



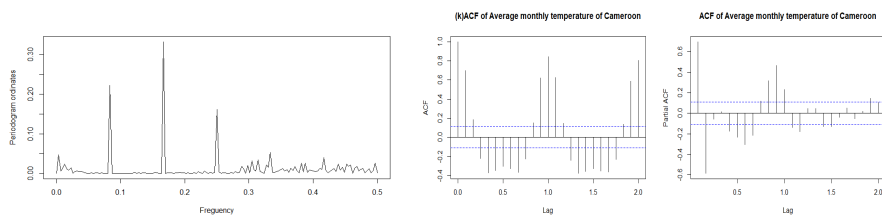
(b) Kenya



(c) Namibia

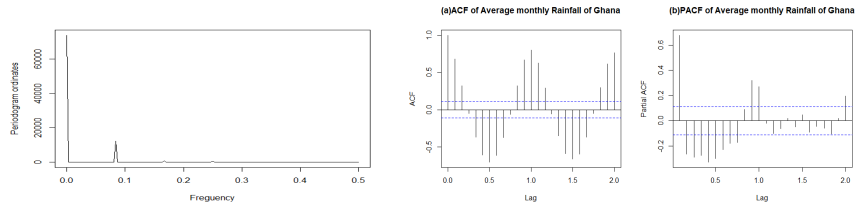


(d) Egypt

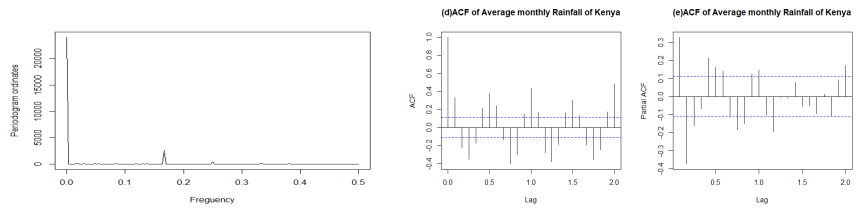


(e) Cameroon

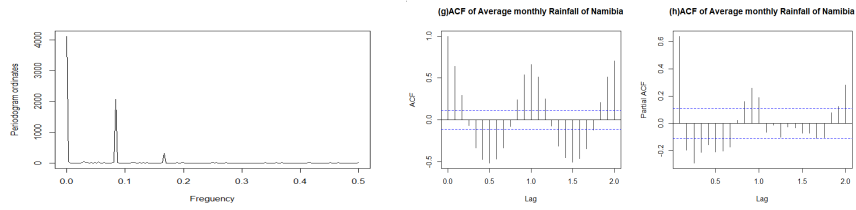
Figure 2: Periodogram and Autocorrelation Analysis of Temperatures Data



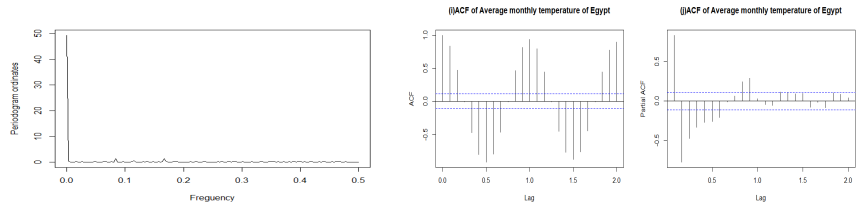
(a) Ghana



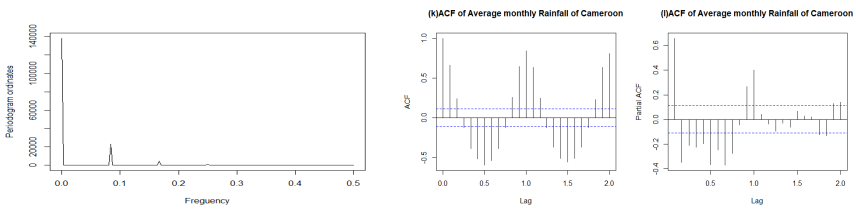
(b) Kenya



(c) Namibia



(d) Egypt



(e) Cameroon

Figure 3: Periodogram and Autocorrelation Analysis of Rainfall Data

Table 2: Model accuracy measures for all formulated models for average monthly temperature

Country	Model	RMSE	Rank	MAE	Rank	MASE	Rank
Ghana	FARIMA(5,1,1,3)(1,0,0)[12]	0.369	2	0.277	1	0.307	1
	SARIMA(1,0,3)(2,1,1)[12]	0.391	1	0.291	2	0.657	2
	NCS	1.440	3	1.223	3	2.757	3
Kenya	FARIMA(3,1,1,3)(0,0,0)	0.407	1	0.320	1	0.474	1
	SARIMA(0,0,2)(0,1,1)[12]	0.443	2	0.343	2	0.735	2
	NCS	0.995	3	0.808	3	1.732	3
Namibia	FARIMA(1,1,1,4)(0,0,2)[12]	0.923	2	0.737	2	0.416	1
	SARIMA(2,0,1)(2,1,1)[12]	0.799	1	0.607	1	0.702	2
	NCS	3.530	3	3.127	3	3.613	3
Egypt	FARIMA(2,5,1,2)(0,0,1)[12]	0.975	1	0.770	1	0.266	1
	SARIMA(2,0,2)(2,1,0)[12]	1.042	2	0.789	2	0.721	2
	NCS	5.982	3	5.347	3	4.887	3
Cameroon	FARIMA(3,1,1,1)(1,0,0)[12]	0.357	1	0.280	1	0.390	1
	SARIMA(1,0,1)(2,1,0)[12]	0.394	2	0.303	2	0.691	2
	NCS	1.123	3	0.951	3	2.168	3

Table 3: Model accuracy measures for all formulated models for average monthly rainfall

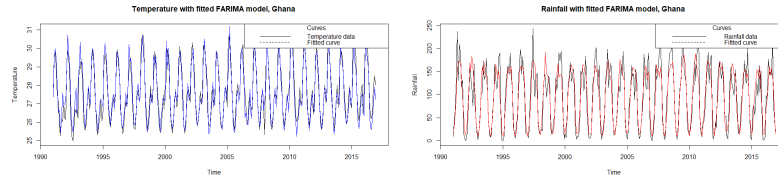
Country	Model	RMSE	Rank	MAE	Rank	MASE	Rank
Ghana	FARIMA(1,0,0,1)(2,0,0)[12]	29.227	1	22.319	1	0.565	1
	SARIMA(1,0,0)(1,1,0)[12]	31.612	2	23.256	2	0.872	2
	NCS	61.496	3	54.561	3	1.381	3
Kenya	FARIMA(1,0,0,1)(2,0,0)[12]	30.462	1	21.688	1	0.655	1
	SARIMA(1,0,0)(1,1,0)[12]	31.569	2	21.970	2	0.774	2
	NCS	36.846	3	29.324	3	0.886	3
Namibia	FARIMA(2,1,0,1)(2,0,1)[12]	14.993	1	8.408	2	0.571	1
	SARIMA(1,0,3)(2,1,2)[12]	14.994	1	8.213	1	0.679	2
	NCS	27.613	3	21.458	2	1.456	3
Egypt	FARIMA(2,0,0,0)(1,0,0)[12]	2.114	1	1.317	1	0.664	1
	SARIMA(3,0,2)(2,0,1)[12]	2.255	3	1.502	3	0.847	2
	NCS	2.149	2	1.500	2	0.756	3
Cameroon	FARIMA(2,0,0,3)(1,0,0)[12]	34.895	1	25.282	1	0.459	1
	SARIMA(0,0,0)(2,1,0)[12]	37.103	2	25.585	2	0.798	2
	NCS	87.165	3	74.770	3	1.358	3

of the formulated models; viz: FARIMA, SARIMA and NCS. A periodogram is used to detect the principal periods (or frequencies) of a time series. This

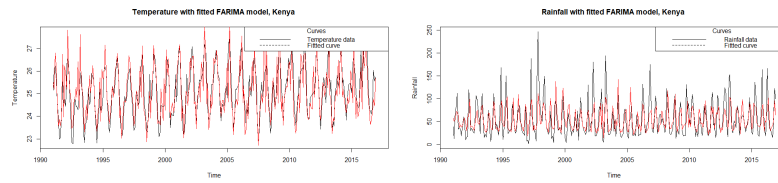
can be a useful means for detecting the main repeated compartment in a series. The periodogram graphs a degree of the relative significance of potential frequency values that might explain the oscillation pattern of the observed data. From the Figures 2, 3, Table 2, and Table 3, for the selected sites, a careful scrutiny to identify the dominant frequencies inherent in the data, the ordinary, and the seasonal terms and orders identified, for example, considering Ghana, the most dominant frequencies,  $K = 5$ ,  $p = 1$ ,  $d = 1$ ,  $q = 3$ ,  $P = 1$ ,  $D = 0$ ,  $Q = 0$ , and  $s = 12$ , thus  $FARIMA(5, 1, 1, 3)(1, 0, 0)_{[12]}$  for average monthly temperature whereas the  $FARIMA(1, 0, 0, 1)(2, 0, 0)_{[12]}$  was identified for average monthly temperature as compared with the natural cubic spline, NCS. The error measures RMSE, MAE, and MASE are also computed. Using MASE, the model with the smallest value, 0.307, is best fitted model for average monthly temperature for Ghana and the smallest value, 0.565, is the best fitted model for average monthly rainfall. For, seasonal ARIMA modeling,  $SARIMA(1, 0, 3)(2, 1, 1)_{[12]}$  was identified for average monthly temperature, and  $SARIMA(1, 0, 0)(1, 1, 0)_{[12]}$  identified for the average monthly rainfall. In general, FARIMA process shows potential adequacy in fitting both average monthly temperature and rainfall for selected study regions, Ghana, Kenya, Namibia, Egypt and Cameroon climatic regions. Comparing results from Tables 2 and 3, among the three models, the natural cubic spline performed less satisfactory and the Fourier function ARIMA, FARIMA, performed most satisfactorily. Based on the analysis, a plot of the original data sets and the best fitted models are in Figure 4. Its shows how well FARIMA modeling adequately models the average monthly temperature and average monthly rainfall.

## 5 Conclusions

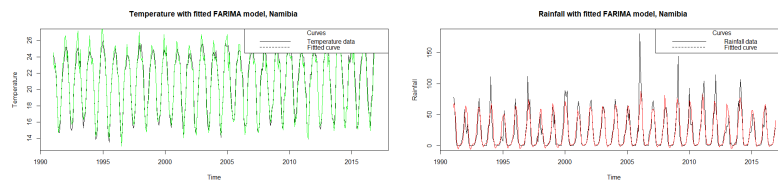
The statistical analysis demonstrates that the average monthly temperature data and average monthly rainfall from the considered five African climatic regions display seasonal variation and dynamics, hence some statistical parameters differ significantly concerning these locations. Again, average monthly temperature and rainfall modeling and fitting presents a stimulating assignment for controlling monthly time series data. Our study has shown that FARIMA models can adequately explain the sequence of the temperature and



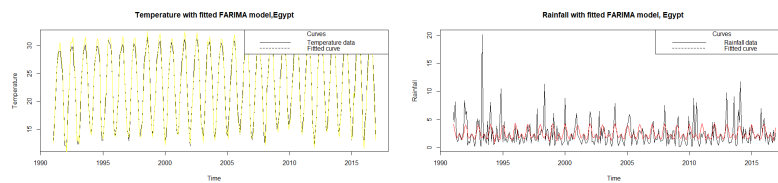
(a) Ghana



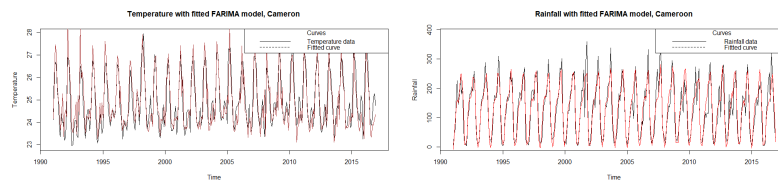
(b) Kenya



(c) Namibia



(d) Egypt



(e) Cameroon

Figure 4: A plot of the original data sets and the best fitted models of Temperature and Rainfall Data

rainfall patterns in the selected climatic regions, generating the smallest mean absolute scaled error. Accordingly, it is recommended, that FARIMA modeling could be considered for modeling temperature and rainfall, to aid as a tool for proper planning on decisions regarding environmental and agricultural models that depends on temperature and rainfall patterns.

## References

- [1] J. Krzyszczak, P. Baranowski, M. Zubik and H. Hoffmann, Temporal scale in uence on multifractal properties of agro-meteorological time series, *Agricultural and Forest Meteorology*, **239**, (2017), 223–235.
- [2] T. Thi Kieu Tran, T. Lee, J.-Y. Shin, J.-S. Kim and M. Kamruzzaman, Deep learning-based maximum temperature forecasting assisted with meta-learning for hyperparameter optimization, *Atmosphere*, **11**(5), (2020), 487.
- [3] M. Adem, N. Solomon, S. Movahhed Moghaddam, A. Ozunu and H. Azadi, The nexus of economic growth and environmental degradation in Ethiopia: time series analysis, *Climate and Development*, (2020), 1–12.
- [4] S. Ansah, M. Ahiataku, C. Yorke, F. Otu-Larbi, B. Yahaya, P. Lamptey and M. Tanu, Meteorological analysis of foods in Ghana, *Advances in Meteorology*, **2020**, (2020).
- [5] Y. Asamoah and K. Ansah-Mensah, Temporal description of annual temperature and rainfall in the bawku area of Ghana, *Advances in Meteorology*, **2020**, (2020).
- [6] E.L. Molua, Climatic trends in Cameroon: implications for agricultural management, *Climate Research*, **30**(3), (2006), 255–262.
- [7] Y.D. Ngondjeb, Agriculture and climate change in cameroon: An assessment of impacts and adaptation options, *African Journal of Science, Technology, Innovation and Development*, **5**(1), (2013), 85–94.

- [8] F. Nyangito and M. Wasonga, Trend analysis of rainfall and temperature variability in arid environment of turkan, Kenya. *Environ*, (2014).
- [9] N. A. Kgabi, M. Uugwanga, J. Ithindi, Atmospheric conditions and precipitation in arid environments: A case of namibia, *International Journal*, **6**(1), (2016), 148–159.
- [10] R. M. El-Hagrsy<sup>1</sup>, T. A. Gado, I. Rashwan, Climate change effects on annual rainfall characteristics in Egypt, (2018).
- [11] G.L. Muhati, D. Olago, L. Olaka, Past and projected rainfall and temperature trends in a sub-humid montane forest in northern kenya based on the cmip5 model ensemble, *Global Ecology and Conservation*, **16**, (2018), e00469.
- [12] B.M. Abdel-Maksoud, Estimation of air temperature and rainfall trends in Egypt, *Asian Journal of Advanced Research and Reports*, (2018), 1–22.
- [13] B.A. Abura, P.O. Hayombe and W.K. Tonui, Rainfall and temperature variations overtime (1986-2015) in Siaya County, Kenya, (2017).
- [14] S. Agrawala, A. Moehner, M. El Raey, D. Conway, M. Van Aalst, M. Hagenstad and J. Smith, Development and climate change in egypt: focus on coastal resources and the Nile, *Organisation for Economic Co-operation and Development*, (2004).
- [15] P. Asare-Nuamah and E. Botchway, Understanding climate variability and change: analysis of temperature and rainfall across agroecological zones in Ghana, *Heliyon*, **5**(10), (2019), e02654.
- [16] S. Awala, K. Hove, M. Wanga, J. Valombola and O. Mwandemele, Rainfall trend and variability in semi-arid northern Namibia: Implications for smallholder agricultural production, *Welwitschia International Journal of Agricultural Sciences*, **1**, (2019), 1–25.
- [17] Frederic and T. Mesmin, Rainfall variability and oods occurrence in the city of Bamenda (Northwest of Cameroon), *Present Environment and Sustainable Development*, **11**(1), (2017), 65–82.

- [18] A. Abdul-Aziz, M. Anokye, A. Kwame, L. Munyakazi, N. Nsowah-Nuamah, et al., Modeling and forecasting rainfall pattern in Ghana as a seasonal arima process: The case of ashanti region, *International Journal of Humanities and Social Science*, **3**(3), (2013), 224–233.
- [19] E. Afrifa-Yamoah, B. Saeed and A. Karim, Sarima modelling and forecasting of monthly rainfall in the Brong Ahafo Region of Ghana, *World Environment*, **6**(1), (2016), 1–9.
- [20] O. Ebhuoma, M. Gebreslasie, L. Magubane, A Seasonal Autoregressive Integrated Moving Average (SARIMA) forecasting model to predict monthly malaria cases in Kwazulu-Natal, South Africa, *South African Medical Journal*, **108**, (2018).
- [21] M. Asamoah-Boaheng, Using SARIMA to forecast monthly mean surface air temperature in the Ashanti Region of Ghana, *International Journal of Statistics and Applications*, **4**(6), (2014), 292–298.
- [22] T.N. Filder, M. M. Muraya, R. M. Mutwiri, Application of seasonal autoregressive moving average models to analysis and forecasting of time series monthly rainfall patterns in embu county, Kenya, *Asian Journal of Probability and Statistics*, (2019) 1–15.
- [23] W. Morishima and I. Akasaka, Seasonal trends of rainfall and surface temperature over Southern Africa, (2010).
- [24] I. Aninagyei and D.O. Appiah, Analysis of rainfall and temperature effects on maize and rice production in Akim Achiase, Ghana, (2014).
- [25] A.W. Maina, W.W. Ronald and T. Richard, Time series analysis modelling of rainfall patterns in Nakuru, Kenya, *International Journal of Social Science and Technology*, **4**(3), (2019).
- [26] P.R. Winters, Forecasting sales by exponentially weighted moving averages, *Management science*, **6**(3), (1960), 324–342.
- [27] G.M.J. George and E.P. Box, *Time Series Analysis: Forecasting and Control* (Revised Edition), Holden-Day, revised edition, 1976.

- [28] A.C. Harvey, *Forecasting, structural time series models and the Kalman filter*, Cambridge University Press, 1990.
- [29] R. Hyndman, A.B. Koehler, J.K.Ord, R.D. Snyder, *Forecasting with exponential smoothing: the state space approach*, Springer Science & Business Media, 2008.
- [30] R.J. Hyndman and A.B. Koehler, Another look at measures of forecast accuracy, *International journal of forecasting*, bf 22(4), (2006), 679–688.
- [31] M. Chonge, K. Nyongesa, O. Mulati, L. Makokha and F. Tireito, A time series model of rainfall pattern of uasin gishu county, *IOSR Journal of Mathematics*, **11**, (2015), 77–84.
- [32] K. Goswami, J. Hazarika, A. Patowary, Monthly temperature prediction based on arima model: A case study in dibrugarh station of assam, india., *International Journal of Advanced Research in Computer Science*, **8**, (2017).